On the Reduction of the Number of Spurious Modes in the Vectorial Finite-Element Solution of Three-Dimensional Cavities and Waveguides

A. KONRAD, SENIOR MEMBER, IEEE

Abstract —A novel approach to the solution of three-dimensional microwave cavity and waveguide problems by finite elements reduces the number of spurious, nonphysical modes. Solutions are obtained in terms of the field vector $\boldsymbol{H}$. Three-dimensional vector boundary conditions are implemented in a way that allows arbitrarily-shaped curved boundaries to be modeled. The formulation is based on a subparametric finite element with 27 interpolation nodes.

I. Introduction

One-component vector formulations have been successful in the solution of two-dimensional waveguides [11] and axisymmetric cavities [2] with an arbitrary cross section. However, when two or more vector components are involved, the spectrum of eigensolutions contains a large number of spurious, nonphysical modes [3], [4]. The spurious modes occur regardless what combination of vector components are involved (e.g., longitudinal $\boldsymbol{E}$ and $\boldsymbol{H}$ vector components [5]–[7], three $\boldsymbol{H}$ vector components [8], etc.), or whether the finite-difference [9] or finite-element methods [10] are employed.

Three-dimensional multicomponent vector formulations are similarly plagued by the occurrence of spurious modes, though this is not always reported [11]. Explanations for the appearance of spurious modes and suggested methods to eliminate the nonphysical solutions are a recurring theme in technical papers on numerical methods for the analysis of microwave devices [3], [4], [6]–[10], [13]. Claims that spurious modes can be eliminated by adding a penalty term to a functional are clearly unacceptable since no reduction occurs in the size of the matrix eigenvalue problem [13]. What happens is that the nonphysical modes are pushed toward higher frequencies and therefore do not show up among the first few physically meaningful modes.

In most three-dimensional methods previously published, the boundary conditions are implemented such that they impose severe restrictions on the cavity shapes that can be analyzed [10]–[12]. Three-dimensional finite-element models are constructed so that boundary conditions can be effortlessly applied. This usually means that the boundary surfaces must be aligned with the Cartesian coordinate planes. The method presented here offers the opportunity to break away from this restriction on cavity shape and orientation. At the same time, since the new approach treats principal vector boundary conditions as constraints, it has the beneficial effect of truly eliminating some of the nonphysical solutions.

Manuscript received April 24, 1985; revised September 19, 1985.
The author is with the General Electric Company, Corporate Research and Development, Schenectady, NY 12301.
IEEE Log Number 8406470.

II. Variational Formulation

The approach described in this paper reduces the size of the matrix eigenvalue problem and thus a great number, though not all, of the spurious solutions are indeed eliminated. Consider the vector Helmholtz's equation given by

$$\operatorname{div} \frac{1}{\epsilon} \operatorname{grad} \boldsymbol{H} + k^2 \mu \boldsymbol{H} = 0 \tag{1}$$

where $\boldsymbol{H}$ is the magnetic field vector, k is the wavenumber, ϵ is permittivity, and μ is permeability.

An associated functional can be written as

$$F(\boldsymbol{h}) = + \iiint \left\{ \frac{1}{\epsilon} |\operatorname{grad} h|^2 - k^2 \mu h^2 \right\} dV - \oiint \left\{ \frac{1}{\epsilon} h \operatorname{grad} h - \boldsymbol{h} \times \frac{1}{\epsilon} \operatorname{curl} \boldsymbol{h} \right\} \cdot \boldsymbol{n} \, dS \tag{2}$$

where $\boldsymbol{h}$ is the trial function for $\boldsymbol{H}$ and $\boldsymbol{n}$ denotes the outward normal unit vector to the boundary surface. Wherever h appears as a scalar in (2), a summation over each component should be understood.

The above variational formulation should be compared with that based on the curlcurl equation, which automatically couples the vector components without need for a surface integral term in the associated functional [4].

III. Boundary Conditions

The *natural* boundary condition of (2) is given by

$$\boldsymbol{n} \times \frac{1}{e} \operatorname{curl} \boldsymbol{h} = 0. \tag{3}$$

This condition is equivalent to normal $\boldsymbol{E}$ field at perfect electric-conductor boundaries. Unfortunately, this does not

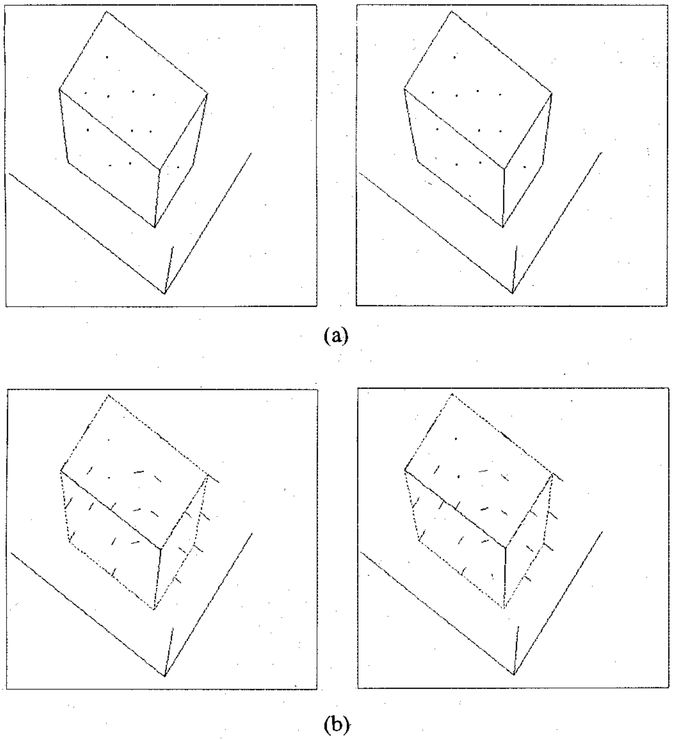

Fig. 1. (a) Stereoscopic image of one quadrant of a rectangular cavity of dimensions $2\times3\times1$ as modeled by a single twenty-seven-noded element. (b) Stereoscopic image of the first mode of the rectangular cavity of Fig. 1(a) showing the magnetic-field vector at the interpolation nodes.

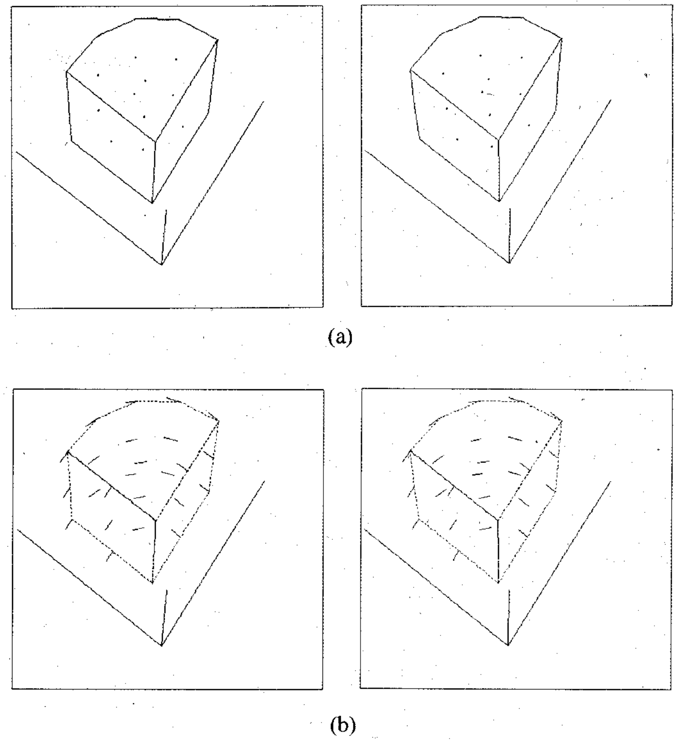

Fig. 2. (a) Stereoscopic image of one quadrant of a circular cylindrical cavity of unit radius as modeled by one finite element. (b) Stereoscopic image of the magnetic-field distribution of the dominant mode in the cylindrical cavity of Fig. 2(a).

guarantee that the magnetic-field vector components will satisfy the other electromagnetic boundary condition, namely

$$\boldsymbol{n}\cdot\boldsymbol{h}=0. \qquad (4)$$

The new method employs (4) as a *principal* boundary condition on the same perfect electric conductor boundary where the natural boundary condition (3) is satisfied. Both natural and principal boundary conditions contribute to the coupling of the three components of $\boldsymbol{h}$.

In most practical three-dimensional cavity and waveguide problems, symmetry can be exploited to reduce the matrix size. Symmetry planes in electromagnetics act like perfect magnetic-conductor boundaries where $\boldsymbol{h}$ must be normal to the surface. This can also be expressed as a *principal* boundary condition given by

$$\boldsymbol{n}\times\boldsymbol{h}=0. \qquad (5)$$

In addition, the homogeneous Neumann boundary condition

$$\boldsymbol{n}\cdot\operatorname{grad} h=0 \qquad (6)$$

is valid for symmetry planes. It is implemented as another *natural* boundary condition by neglecting the surface integral term from (2).

IV. Finite-Element Method

Conditions (4) and (5) imply that the components of $\boldsymbol{h}$ are not linearly independent. Without (4) and (5), a finite-element solution based on (2) would yield many spurious, nonphysical solutions. Principal boundary conditions are applied *after* functional discretization and minimization have been performed. The result is a reduction in the size of the global coefficient matrices and, hence, the elimination of many nonphysical modes from the spectrum. The algorithmic implementation is based on the concept of rectangular finite-element connection matrices.

Each unknown vector component is approximated by 27 Lagrange interpolation polynomials. The shape of the element is described by a different set of 26 interpolation polynomials associated with the nodes at the surface of the element. The Jacobian matrix of transformation between local and global coordinates is used to evaluate the global derivatives appearing in (2) in terms of the local derivatives. A 27-point Gaussian quadrature formula is employed for volume integration, and a 9-point formula is used for surface integration.

V. Examples

Fig. 1(a) shows the stereoscopic image of one *quadrant* of a *rectangular* cavity of dimensions $2\times3\times1$ as modeled by a single element. Fig. 1(b) shows the stereoscopic image of the first resonant mode. The computed wavenumber of 1.89495 compares very well (0.37 percent error) with the analytical solution of 1.88786.

Ordinarily, a three-component vector solution using 27 finite-element nodes yields a 81×81 matrix eigenvalue problem with the majority of the 81 eigensolutions being nonphysical. The application of (4) and (5) reduces the matrix size to 28, thereby eliminating 53 spurious solutions.

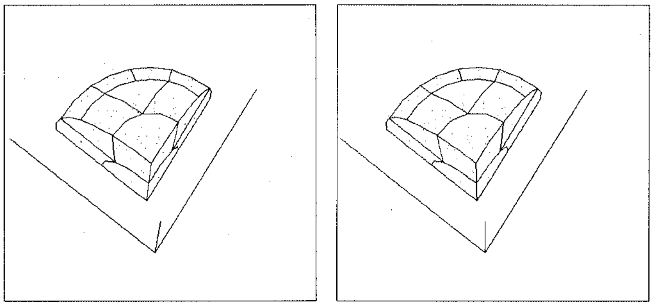

(a)

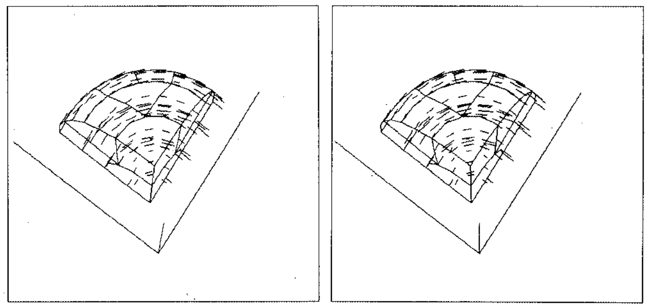

(b)

Fig. 3. (a) Stereoscopic image of one octant of a spherical cavity of unit radius as modeled by eight twenty-seven-noded elements. (b) Stereoscopic image of the magnetic-field distribution of the lowest order mode in the spherical cavity of Fig. 3(a).

Fig. 2(a) shows one *quadrant* of a circular *cylindrical* cavity of unit height and radius modeled by one finite element. Fig. 2(b) shows the 3D stereoscopic picture of the dominant mode. The computed wavenumber is 2.47181, the analytical solution is 2.40482. The 2.78-percent error is reasonable considering that the finite-element model consists of just one extremely distorted brick element. The matrix size for this problem was 31.

Fig. 3(a) shows one *octant* of a *spherical* cavity of unit radius, modeled by eight elements (125 interpolation nodes). Fig. 3(b) shows the ***H***-field distribution of the dominant mode. The finite-element solution for the wavenumber is 2.80584, a very good approximation (0.27-percent error) to the analytical solution (2.79839). The matrix size for this problem would be 375 if the principal boundary conditions were not enforced. The actual matrix size was 220.

VI. Conclusions

Comparing the present method with the one based on the curlcurl equation, one should notice that the approach for *axisymmetric* cavities described in [4] incorporates the natural boundary condition (3) but not the principal boundary condition (4). Without the principal boundary condition (4), the two formulations are mathematically equivalent and yield both the physically meaningful as well as a great number of spurious solutions. The present formulation yields the same physically meaningful solutions, plus a series of spurious solutions. However, since the matrix size is smaller, the number of spurious solutions is less. The authors of [4] have also noticed that by enforcing the principal boundary condition (4) "some spurious solution eigenvalues are indeed eliminated, but not all."

The results obtained with the one-element models are testimony to the versatility of the twenty-seven-noded subparametric element and the accuracy and correctness of the present approach. The examples shown in Figs. 1(b) and 2(b) were chosen because of the exceptional clarity of the pictures. The spherical cavity example given in Fig. 3(b) shows that principal boundary conditions on curved surfaces can also be enforced in multi-element models.

References

[1] P. Silvester, "A general high-order finite element waveguide analysis program," *IEEE Trans. Microwave Theory Tech.*, vol. MTT-17, pp. 204–210, 1969.

[2] A. Konrad, "Linear accelerator cavity field calculation by the finite element method," *IEEE Trans. Nucl. Sci.*, vol. NS-20, pp. 802–808, 1973.

[3] A. Konrad, "Vector variational formulation of electromagnetic fields in anisotropic media," *IEEE Trans. Microwave Theory Tech.*, vol. MTT–24, pp. 553–559, 1976.

[4] J. B. Davies, F. A. Fernandez, and G. Y. Philippou, "Finite element analysis of all modes in cavities with circular symmetry," *IEEE Trans. Microwave Theory Tech.*, vol. MTT-30, pp. 1975–1980, 1982.

[5] Z. J. Csendes and P. Silvester, "Numerical solution of dielectric loaded waveguides: I—Finite-element analysis," *IEEE Trans. Microwave Theory Tech.*, vol. MTT-18, pp. 1124–1131, 1970.

[6] M. Ikeuchi, K. Inoue, H. Sawami, and H. Niki, "Spurious solutions in the finite-element analysis of microstrip lines," *Elec. Eng. Japan*, vol. 98, pp. 8–15, 1978.

[7] N. Mabaya, P. E. Lagasse, and P. Vanden, "Finite element analysis of optical waveguides," *IEEE Trans. Microwave Theory Tech.*, vol. MTT-29, pp. 600–605, 1981.

[8] B. M. A. Rahman and J. B. Davies, "Finite-element analysis of optical and microwave waveguide problems," *IEEE Trans. Microwave Theory Tech.*, vol. MTT-32, pp. 20–28, 1984.

[9] D. G. Corr and J. B. Davies, "Computer analysis of the fundamental and higher order modes in single and coupled microstrip," *IEEE Trans. Microwave Theory Tech.*, vol. MTT-20, pp. 669–678, 1972.

[10] M. Hara, T. Wada, T. Fukasawa, and F. Kikuchi, "A three dimensional analysis of RF electromagnetic fields by the finite element method," *IEEE Trans. Magn.*, vol. MAG-19, pp. 2417–2420, 1983.

[11] R. L. Ferrari and G. L. Maile, "Three-dimensional finite-element method for solving electromagnetic problems," *Electron. Lett.*, vol. 14, pp. 467–468, 1978.

[12] J. P. Webb, G. L. Maile, and R. L. Ferrari, "Finite-element solution of three-dimensional electromagnetic problems," *Proc. Inst. Elec. Eng.*, vol. 130, pt. H, no. 2, pp. 153–159, Mar. 1983.

[13] M. Koshiba, K. Hayata, and M. Suzuki, "Vectorial finite-element method without spurious solutions for dielectric waveguide problems," *Electron. Lett.*, vol. 20, pp. 409–410, 1984.

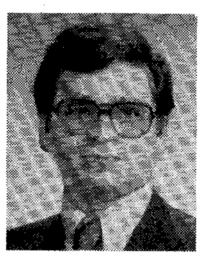

A. Konrad (S'70–M'75–SM'84) was born on February 15, 1946. From 1970 to April 1975, he was a graduate student and research assistant with the Department of Electrical Engineering at McGill University, Montreal, P. Q., Canada. During these years, he was involved in the application of the finite-element method to the solution of electromagnetic-field problems. In April 1972, he won first prize in the Canada-wide graduate student paper competition of the Canadian Nuclear Association with the paper entitled "Linear Accelerator Cavity Field Calculation by the Finite Element Method" (*IEEE Trans. Nucl. Sci.*, vol. NS-20, pp. 802–808, 1973). He received the B.Eng., M.Eng., and Ph.D. degrees in 1970, 1971, and January 1975, respectively.

During the summer of 1975, he was a Visiting Researcher at the Institut National Polytechnique de Grenoble, Grenoble, France, where he worked on the development of three-dimensional finite-element programs for electrostatic problems. He was employed by the National Research Council, Ottawa, Ont., Canada, from August 1975 to November 1979, as an Assistant Research Officer in the Division of Building Research. During this time, he worked on various aspects of solar energy research and computer simulation techniques for the study of air infiltration and energy consumption of small residential buildings in Canada. Since joining General Electric in December 1979, he has been responsible for the development of finite-element methods and computer programs for the numerical solution of magnetostatic, eddy-current, and skin-effect problems with applications to transformers and motors. His current interests include ceramic chip carrier network analysis, microwave integrated-circuit field analysis, RF scattering problems, and antenna design.

Since 1971, Dr. Konrad has authored or coauthored over 40 publications. He is a member of the Association of Professional Engineers of the Province of Ontario. Presently, he is serving as Vice Chairman (Programs) of the Schenectady Section of the IEEE.